

# Local versus Global Two-Photon Interference in Quantum Networks

Thomas Nitsche,<sup>1</sup> Syamsundar De,<sup>1,\*</sup> Sonja Barkhofen,<sup>1</sup> Evan Meyer-Scott,<sup>1</sup>  
Johannes Tiedau,<sup>1</sup> Jan Sperling,<sup>1</sup> Aurél Gábris,<sup>2,3</sup> Igor Jex,<sup>2</sup> and Christine Silberhorn<sup>1</sup>

<sup>1</sup>Applied Physics, Paderborn University, Warburger Straße 100, 33098 Paderborn, Germany

<sup>2</sup>Department of Physics, Faculty of Nuclear Sciences and Physical Engineering,

Czech Technical University in Prague, Břehová 7, 115 19 Praha 1–Staré Město, Czech Republic

<sup>3</sup>Wigner Research Centre for Physics, Konkoly-Thege M. út 29–33, H-1121 Budapest, Hungary

(Dated: August 29, 2022)

We devise an approach to characterizing the intricate interplay between classical and quantum interference of two-photon states in a network, which comprises multiple time-bin modes. By controlling the phases of delocalized single photons, we manipulate the global mode structure, resulting in distinct two-photon interference phenomena for time-bin resolved (local) and time-bucket (global) coincidence detection. This coherent control over the photons' mode structure allows for synthesizing two-photon interference patterns, where local measurements yield standard Hong-Ou-Mandel dips while the global two-photon visibility is governed by the overlap of the delocalized single-photon states. Thus, our experiment introduces a method for engineering distributed quantum interferences in networks.

*Introduction.*—The naive idea that our world consists of particles, reminiscent of tiny billiard balls, which govern the laws of physics has been refuted. Rather, it is waves, be it classical or quantum, which describe nature best—covering areas ranging from gravity to hydrodynamics to optics to subatomic systems. For example, quantum field theories merely consider elementary particles as excitations of an underlying, fundamental quantum field, such as photons for light [1]. Thus, even particles must be able to interfere, which was demonstrated, e.g., in double-slit experiments with electrons [2]. To speak of genuine quantum interference, we must consider at least two particles, like in the seminal Hong-Ou-Mandel (HOM) effect in the interference of two photons [3]. With recent theoretical and technological advances in the control of quantum systems, there is a spur of interest in how such multiparticle interferences can manifest themselves in large networks [4].

Since interference is ubiquitous, techniques to generate, characterize, tailor, and exploit such phenomena have been developed, together known as coherent control [5]. Classical applications of coherent control include spectroscopy, chemistry, and various imaging techniques. In addition, the recent strong demand for developing efficient solutions for coherent control of large quantum systems arose from innovations in quantum information processing and technologies that exploit quantum coherence to its full extent [6–8].

Photonic networks provide an excellent platform for studying large-scale coherence effects [9]. For both practical and fundamental purposes, the quality of a network—benchmarked by stability, scalability, and reconfigurability—mainly depends on its coherence and control properties. In addition, networks allow for a natural distinction of local and global features, and the introduction of multiple quantum particles to passive networks is key to many quantum communication schemes [7]. Earlier studies aimed at manipulating coherence of photons to alter the fundamental HOM effect [10], exposing in an intricate connection of classical and quantum interference [11–14]. However, the fundamentals of the inter-

play of local and global coherences, including its active control, remain widely unexplored.

In this letter, we use coherent control over single photons, spread over multiple nodes of a network, to demonstrate how their superposition state affects quantum interference patterns. We put forward correlation measures which certify the presence of two-particle quantum coherence across a linear optical network for probing local versus global coherence. Our implementation employs a time-bin-multiplexing architecture with a compatible source of photons and configurable measurement for accessing various types of correlations. Identifying local and global correlations enables us to study contributions of the coherence properties of the source and non-local coherence properties of the network.

*Controlling and observing two-photon interference.*—We outline our approach in Fig. 1(a). The core of our system is a mode synthesizer which allows us to individually shape the time-bin mode structure of photons and, thereby, their interference characteristics. This is implemented using a linear photonic network, its crucial feature being reconfigurability. The realization of a mode synthesizer requires the ability to coherently manipulate selected degrees of freedom, such as polarisation, frequency, or time-bin modes. Naturally, suitable single-photon sources and detectors must be available too.

Our experiments use a time-multiplexing fibre loop setup that provides a resource-efficient, scalable, stable, and flexible platform for the implementation of networks, and which has been used, among others, to realize quantum walks [15–18] and boson sampling [18–21]. The mode synthesis phase of our experiment is implemented by employing fast modulators and stable delay lines, resulting in each photon being coherently spread over multiple time bins. In the analysis phase, the photons are brought to interference and measured with detectors capable of resolving individual time bins. Coincidence events at the same time-bin allow for assessing local correlations, and combined coincidences across multiple time-bins are used for extracting global correlations [cf. Fig. 1(b)].

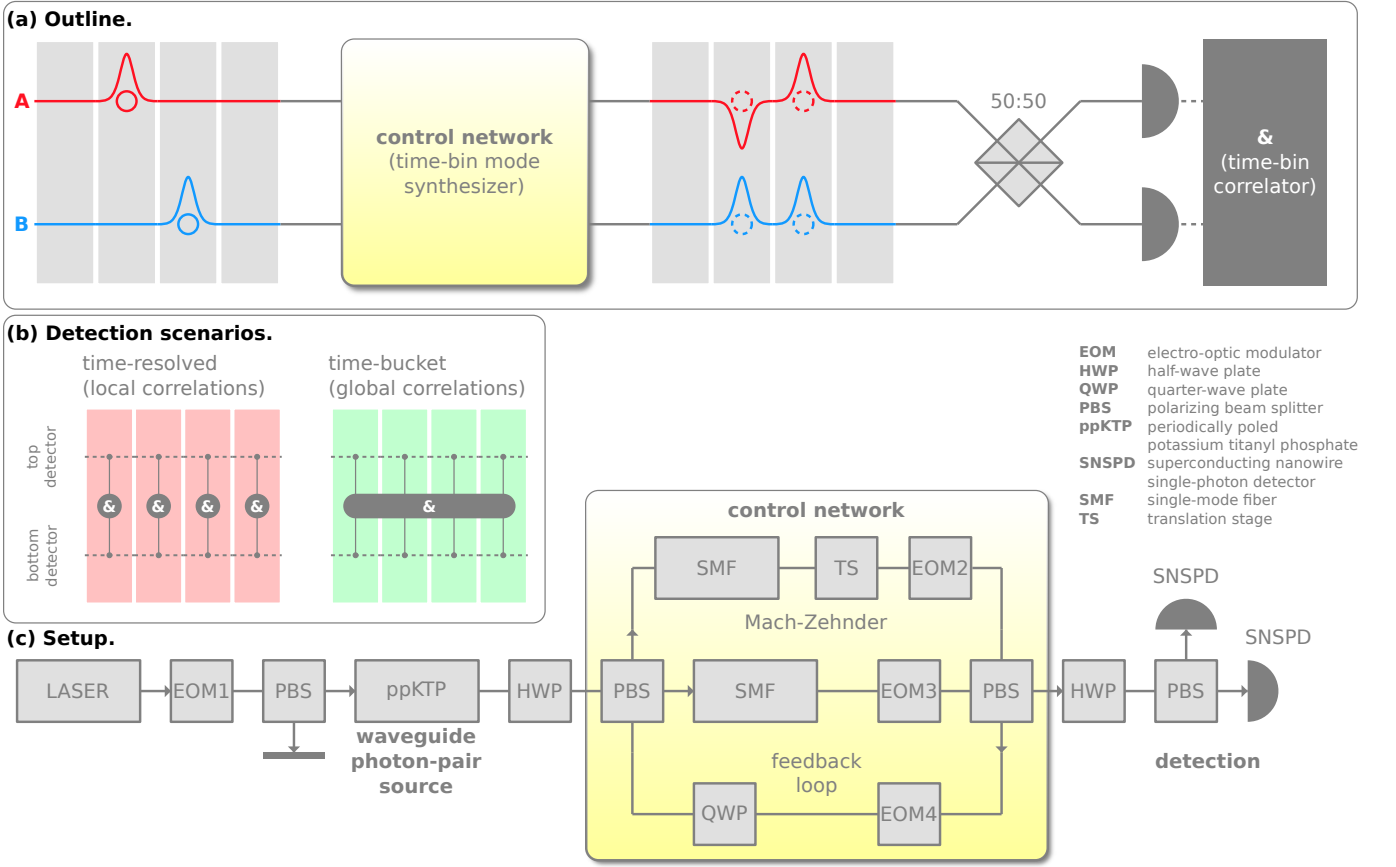


FIG. 1. (a) Two-photon interference protocol. Photons  $A$  and  $B$  are generated in different (time-bin) modes. Using a highly reconfigurable network, we synthesize arbitrary mode structures over which the photons are coherently distributed. In a subsequent HOM configuration, the two photons are superimposed, and correlations are measured. (b) Illustration of the two fundamentally different measures of correlation. Local correlations involve signals from the top and bottom detectors at the same time bin, while global correlations access coincidences across multiple time-bins. (c) Schematics of our setup. Our setup comprises state-of-the-art building blocks: a compatible photon source, a flexible control network (implemented as a time-multiplexed Mach-Zehnder interferometer with a feedback loop and deterministic in- and out-coupling), and a versatile detection stage.

*Ideal model for local and global correlations.*—Using the standard quantum optics formalism [22], we can introduce a simple theoretical model that describes our system in the absence of imperfections. We label the initial photons as  $A$  and  $B$ , distributed in the control network over time bins as  $\hat{A}^\dagger|\text{vac}\rangle = \sum_\tau \alpha_\tau \hat{a}_\tau^\dagger|\text{vac}\rangle$  and  $\hat{B}^\dagger|\text{vac}\rangle = \sum_\tau \beta_\tau \hat{b}_\tau^\dagger|\text{vac}\rangle$ , where  $\hat{a}_\tau^\dagger$  and  $\hat{b}_\tau^\dagger$  are bosonic creation operators for the modes under study (index  $\tau$ ) and  $\alpha$  and  $\beta$  are the corresponding probability amplitudes. A superposition of these photons on a 50:50 beam splitter results in output modes  $(\hat{a}_\tau \pm \hat{b}_\tau)/\sqrt{2}$ . The output correlations are measured with the top (+) and bottom (−) detector in Fig. 1, represented through photon-number operators  $\hat{n}_{\pm,\tau}$ . This yields the first-order correlation  $G_{\pm,\tau}^{(1)} = \langle \hat{n}_{\pm,\tau} \rangle = (|\alpha_\tau|^2 + |\beta_\tau|^2)/2$ , giving the same values for both detectors, and the second-order cross-correlation

$$G_{\tau,\tau'}^{(1,1)} = \langle \hat{n}_{+,\tau} \hat{n}_{-,\tau'} \rangle = \frac{|\alpha_\tau \beta_{\tau'} - \alpha_{\tau'} \beta_\tau|^2}{4}. \quad (1)$$

To arrive at a refined notion of local and global correlations, we select a set of modes  $\mathbb{S}$ , potentially being a subset

of all network modes. For convenience, we associate the vectors  $\vec{\alpha} = [\alpha_\tau]_{\tau \in \mathbb{S}}$  and  $\vec{\beta} = [\beta_\tau]_{\tau \in \mathbb{S}}$  with the photons  $A$  and  $B$ , respectively. This allows us to identify counts from a single detector,  $G_{\pm}^{(1)} = \sum_{\tau \in \mathbb{S}} G_{\tau}^{(1)} = (\vec{\alpha}^\dagger \vec{\alpha} + \vec{\beta}^\dagger \vec{\beta})/2$ .

Moreover, we arrive at compact formulas for correlation measures which characterize two-photon interference. For any selected set  $\mathbb{S}$  of modes, we introduce the local and global correlation measures as the sums

$$G_{\text{local}}^{(1,1)} = \sum_{\tau \in \mathbb{S}} G_{\tau,\tau}^{(1,1)} \quad \text{and} \quad G_{\text{global}}^{(1,1)} = \sum_{\tau,\tau' \in \mathbb{S}} G_{\tau,\tau'}^{(1,1)}, \quad (2)$$

respectively. Using (1), these correlations then obey

$$G_{\text{local}}^{(1,1)} = 0 \quad \text{and} \quad G_{\text{global}}^{(1,1)} = \frac{(\vec{\alpha}^\dagger \vec{\alpha})(\vec{\beta}^\dagger \vec{\beta}) - |\vec{\alpha}^\dagger \vec{\beta}|^2}{2}. \quad (3)$$

Expressions for experimentally relevant quantities, such as normalized correlation functions,  $g = G^{(1,1)}/[G_+^{(1)}G_-^{(1)}]$ , and visibilities,  $V = 1 - 2g$ , can be readily obtained.

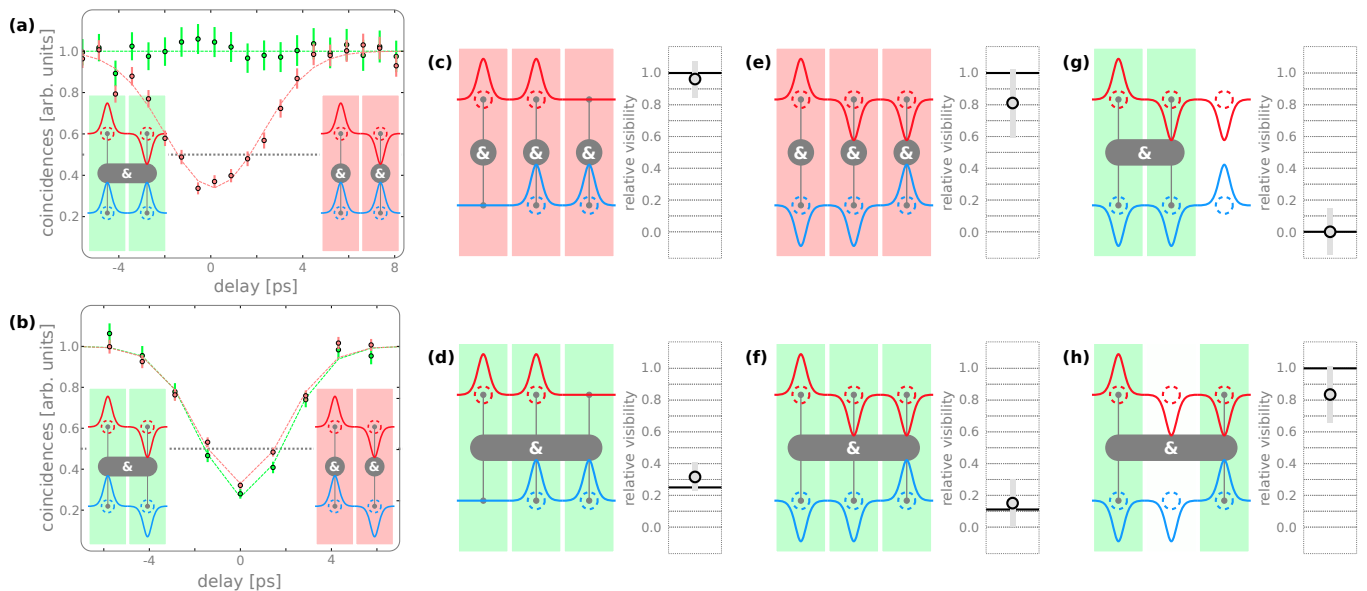


FIG. 2. Two-photon interference patterns for various synthesized mode structures. Plots (a) and (b) depict the interference via coincidences, where red and green data points indicate local and global detection scenarios (see insets). The curves indicate values obtained from a numerical model that includes imperfections, and the dotted line marks the quantum-classical boundary, certifying photon antibunching [23]. The characteristic HOM dip can be observed via local measurements, with visibilities close to the reference value  $V_0 = 0.801 \pm 0.097 > 1/2$ . Global coincidences correspond to the overlap of the synthesized photon modes, showing high two-photon coherence for orthogonal mode structures (b) and no interference for parallel case (a). Plots (c)–(h) depict our results for different multimode interference scenarios. Since  $V_0$  is the dominant limiting factor on all visibilities, a normalization of the visibility (circles including error bars) to this value allows a straightforward comparison to the ideal model (thick solid line).

With this approach, we are able to gain deeper insight into the coherence properties by evaluating the measured coincidences and interference visibilities. Since local correlations,  $G_{\text{local}}^{(1,1)}$ , depend only on the source quality and imperfections of the network, the obtained visibilities relate to photon distinguishability at each time bin separately, exhibiting high visibility for high indistinguishability. Complementing this, global correlations,  $G_{\text{global}}^{(1,1)}$ , are additionally sensitive to the synthesized mode structure by correlating coincidences over multiple time bins.

*Implementation.*—At the core of our experimental setup lies a fiber-based unbalanced Mach-Zehnder interferometer with a feedback loop, as outlined in Fig. 1(c) that serves as a dynamically reconfigurable, time-multiplexing network [24]. The length difference of the single-mode fibers at the two interferometer arms sets the time-bin spacing ( $\sim 105$  ns). A translation stage (TS) allows fine scanning of the time delays in the picosecond regime between the two interfering photons. The network contains fast electro-optic modulators (EOMs), capable of implementing controlled polarization rotations at any time-bin. EOM2 and EOM3 ensure deterministic in- and out-coupling of the photons, whereas EOM4 allows synthesis of complex mode structures by programming appropriate switching patterns.

We implement a type-II parametric down-conversion process in periodically poled potassium titanyl phosphate waveguide as an engineered source of heralded single photons with

high spatial and spectral purity [25]. A picosecond pump laser at 775 nm and a bandwidth of  $\sim 0.3$  nm together with a 2.5 cm long waveguide generates relatively broad ( $\sim 2.7$  ps) photon pulses at telecom wavelength. These picosecond photon pulses barely suffer from the difference in dispersive broadening in the fibers, thus maintain good indistinguishability even after several roundtrips through the network. To ensure that the two interfering photons are generated in desired time-bins, we implement pulse picking on the pump laser using EOM1 and a polarization beam splitter (PBS). As a measure of the source quality, we obtain a visibility of the HOM coincidence count suppression of up to  $V_0 = 0.801 \pm 0.097$ , limited by the residual spectral distinguishability as well as higher photon-number terms in the heralded photon states. This source visibility serves as a reference for discerning interference from mode synthesis from source imperfections.

Our detection scheme consists of two superconducting nanowire single-photon detectors with dead-time and jitter well below the time-bin spacing, together with a PBS for separating the two polarizations, thus allowing both polarization and time-bin resolved measurements.

*Results.*—In Fig. 2, we present the results of our in-depth two-photon interference analysis. In panels (a) and (b), the measured local and global coincidences are plotted against the delay introduced by the TS. Panel (a) corresponds to the case when the photons are distributed over two time bins such that their mode structure is described by two orthogonal vectors  $\vec{\alpha}$

and  $\vec{\beta}$ , while the correlations obtained for photons with identical mode structures are given in panel (b). In both cases, the local correlations behave identically, and with visibilities significantly exceeding the classical threshold, certify local quantum features. Global correlations, however, exhibit a remarkably different behaviour depending on the mode structure of the two photons. For the orthogonal case [Fig. 2(a)], no interference is observed because of a vanishing mode overlap. However, for identical mode structures [Fig. 2(b)], the visibility of interference is roughly equal to those of local correlations, stemming from an almost perfect mode overlap.

To explore the impact of coherent control for more complex mode structures, we synthesized various single-photon states involving three time-bins, Figs. 2(c)–(h). To factor out the effect of initial impurities, we normalize all obtained visibilities by the reference  $V_0$ , and observe remarkably good agreement with the ideal model (thick solid lines).

For Figs. 2(c) and 2(d), we considered photons spreading across two time bins but with a relative offset of a single time bin. This is achieved through our unique control over the parameters  $\vec{\alpha}$  and  $\vec{\beta}$ . This does not change the maximal local interference, panel (c). However, for the resulting reduced overlap between the photon states, our model predicts a reduced global visibility of 25% in panel (d), to which our experimental data agrees with within the error margin. (Errors are obtained from standard statistical error analysis and error propagation.)

In Figs. 2(e)–(h), we depict our results with photons in superposition of three modes. The quality and quantum nature of two-photon interference is certified by local correlations, shown in Fig. 2(e). Cross-correlations between all pairs of time bins, Fig. 2(f), are expected to yield a global visibility of  $1/9 \approx 11\%$  for the generated pulse shapes, again being confirmed by our data. To reveal coherence between parts of the network, we consider correlations restricted to subsets of modes  $\mathbb{S}$ . For instance, when restricted to the first two time bins, the two photons have orthogonal submode structures [Fig. 2(g)], thus yielding no visible interference. However, coincidences from time bins one and three [Fig. 2(h)], in which the photons have identical submode structure (up to a global phase), exhibit quantum coherence limited only by the photons' distinguishability [compare to Fig. 2(e)].

Therefore, these results demonstrate how classical coherent control over the mode synthesizer network can be used to alter global quantum interference across several optical modes. Thus, by tailoring the time-bin-distributed shape of the input quantum light, we can generate and analyze the intricate details of coherent correlations of interfering quantum particles.

*Summary and conclusion.*—In summary, we established a generic scheme for controlling and characterizing local and global coherence effects in the interference of multiple quantum particles. Using a time-multiplexed network for our on-demand mode synthesis, we determined interference visibilities to quantify the amount and kind of quantum coherence imprinted in the temporal distribution of two photons. Thereby, our experiments demonstrate an intricate interplay

between classical mode interference and quantum coherence, and also serve as a benchmark for how classical coherence can be used to govern quantum effects. Beyond purely assessing standard quantum HOM interference, our framework applies to any network architecture for the realization of a manifold of coherences phenomena at will.

In the context of time-multiplexing our concepts can be intuitively related to standard HOM interference, however, the framework is applicable to any network implementation, yielding a powerful tool for realizing and analysing network-wide quantum coherence phenomena.

Our results certify an unprecedented level of control that extends over multiple time bins and which enables us to manipulate quantumness not only locally, but globally. This includes engineering quantum interference between arbitrarily selected parts of the full system. Our coherent control renders it possible to purposefully alter our system towards any desired quantum interference for studying the rich landscape of quantum superpositions. Furthermore, our network has no fundamental restrictions regarding future increments of the number of modes and photons, thus paving the route for applications in photonic quantum information science, such as quantum simulators [26] and remote state preparation protocols [27], which exploit different forms of multi-photon quantum interference phenomena.

*Acknowledgments.*—The Integrated Quantum Optics group acknowledges financial support through the Gottfried Wilhelm Leibniz-Preis (Grant No. SI1115/3-1) and the European Commission through the ERC project QuPoPCoRN (Grant No. 725366). A. G. and I. J. received financial support by the Czech Science foundation (GAČR) project number 17-00844S and by RVO 14000. I. J. acknowledges funding from the project “Centre for Advanced Applied Sciences,” Registry No. CZ.02.1.01/0.0/0.0/16\_019/0000778, supported by the Operational Programme Research, Development and Education, co-financed by the European Structural and Investment Funds and the state budget of the Czech Republic; and A. G. by the National Research Development and Innovation Office of Hungary under project No. K124351.

---

\* [syamsundar.de@upb.de](mailto:syamsundar.de@upb.de)

- [1] R. Loudon, *The quantum theory of light* (Oxford University Press, Oxford, UK, 1973).
- [2] O. Donati, G. P. Missiroli, and G. Pozzi, An experiment on electron interference, *Am. J. Phys.* **41**, 639 (1973).
- [3] C. K. Hong, Z. Y. Ou, and L. Mandel, Measurement of subpicosecond time intervals between two photons by interference, *Phys. Rev. Lett.* **59**, 2044 (1987).
- [4] J.-W. Pan, Z.-B. Chen, C.-Y. Lu, H. Weinfurter, A. Zeilinger, and M. Żukowski, Multiphoton entanglement and interferometry, *Rev. Mod. Phys.* **84**, 777 (2012).
- [5] H. M. Wiseman and G. J. Milburn, *Quantum measurement and control* (Cambridge University Press, Cambridge, UK, 2010).
- [6] A. M. Childs, D. Gosset, and Z. Webb, Universal Computation by Multiparticle Quantum Walk, *Science* **339**, 791 (2013).

- [7] E. Knill, R. Laflamme, and G. J. Milburn, A scheme for efficient quantum computation with linear optics, *Nature (London)* **409**, 46 (2001).
- [8] R. Raussendorf, and H. J. Briegel, A one-way computer, *Phys. Rev. Lett.* **86**, 5188 (2001).
- [9] J. L. O'Brien, A. Furusawa, and J. Vučković Photonic quantum technologies, *Nat. Photon.* **3**, 687 (2009).
- [10] Y. H. Shih and C. O. Alley, New type of einstein-podolsky-rosen-bohm experiment using pairs of light quanta produced by optical parametric down conversion, *Phys. Rev. Lett.* **61**, 2921 (1988).
- [11] P. G. Kwiat, A. M. Steinberg, and R. Y. Chiao, Observation of a quantum eraser: A revival of coherence in a two-photon interference experiment, *Phys. Rev. A* **45**, 7729 (1992).
- [12] T. Legero, T. Wilk, M. Hennrich, G. Rempe, and A. Kuhn, Quantum beat of two single photons, *Phys. Rev. Lett.* **93**, 070503 (2004).
- [13] A. J. Menssen, A. E. Jones, B. J. Metcalf, M. C. Tichy, S. Barz, W. S. Kolthammer, and I. A. Walmsley, Distinguishability and Many-Particle Interference, *Phys. Rev. Lett.* **118**, 153603 (2017).
- [14] M. Rezai, J. Sperling, and I. Gerhardt, What can single photons do what lasers cannot do?, *Quantum Sci. Technol.* **4**, 045008 (2019).
- [15] Y. Aharonov, L. Davidovich, and N. Zagury, Quantum random walks, *Phys. Rev. A* **48**, 1687 (1993).
- [16] A. Schreiber, K. N. Cassemiro, V. Potoček, A. Gábris, P. J. Mosley, E. Andersson, I. Jex, and C. Silberhorn, Photons Walking the Line: A Quantum Walk with Adjustable Coin Operations, *Phys. Rev. Lett.* **104**, 050502 (2010).
- [17] T. Nitsche, S. Barkhofen, R. Kruse, L. Sansoni, M. Štefaňák, A. Gábris, V. Potoček, T. Kiss, I. Jex, and C. Silberhorn, Probing measurement-induced effects in quantum walks via recurrence, *Sci. Adv.* **4**, eaar6444 (2018).
- [18] S. Aaronson and A. Arkhipov, The computational complexity of linear optics, in *Proceedings of the Forty-third Annual ACM Symposium on Theory of Computing, (ACM), STOC 11*, pp. 333–342 (2011).
- [19] K. R. Motes, A. Gilchrist, J. P. Dowling, and P. P. Rohde, Scalable boson sampling with time-bin encoding using a loop-based architecture, *Phys. Rev. Lett.* **113**, 120501 (2014).
- [20] Y. He *et al.*, Time-bin-encoded boson sampling with a single-photon device, *Phys. Rev. Lett.* **118**, 190501 (2017).
- [21] M. Walschaers, Signatures of many-particle interference, *J. Phys. B: At. Mol. Opt. Phys.* **53**, 043001 (2020).
- [22] L. Mandel and E. Wolf, *Optical Coherence and Quantum Optics* (Cambridge University Press, Cambridge, UK, 1995).
- [23] H. J. Kimble, M. Dagenais, and L. Mandel, Photon Antibunching in Resonance Fluorescence, *Phys. Rev. Lett.* **39**, 691 (1977).
- [24] T. Nitsche, F. Elster, J. Novotný, A. Gábris, I. Jex, S. Barkhofen, and C. Silberhorn, Quantum walks with dynamical control: graph engineering, initial state preparation and state transfer, *New. J. Phys.* **18**, 063017 (2016).
- [25] G. Harder, V. Ansari, B. Brecht, T. Dirmeier, C. Marquardt, and C. Silberhorn, An optimized photon pair source for quantum circuits, *Opt. Express* **21**, 13975 (2013).
- [26] A. Aspuru-Guzik and P. Walther, Photonic quantum simulators, *Nat. Phys.* **8**, 285 (2012).
- [27] C. H. Bennett, P. Hayden, D. W. Leung, P. W. Shor, and A. Winter, Remote preparation of quantum states, *IEEE Trans. Inf. Theo.* **51**, 56 (2005).